Excitonic two-photon absorption in semiconducting carbon nanotubes within an effective-mass approximation

Seiji Uryu,[1] Hiroshi Ajiki,[2] and Tsuneya Ando[1]
[1]*Department of Physics, Tokyo Institute of Technology, 2-12-1 Ookayama, Meguro-ku, Tokyo 152-8551, Japan*
[2]*Department of Materials Engineering Science, Osaka University, 1-3 Machikaneyama-cho, Toyonaka, Osaka 560-8531, Japan*
(Received 5 April 2008; revised manuscript received 1 July 2008; published 16 September 2008)

Two-photon absorption associated with excited exciton states is theoretically studied in semiconducting carbon nanotubes within an effective-mass approximation. Sharp absorption peaks appear at energies of the second and fourth lowest exciton states below the interband continuum. The binding energy of the second lowest exciton typically ranges from ~20% to ~40% of that of the lowest exciton depending on the strength of the Coulomb interaction.

DOI: 10.1103/PhysRevB.78.115414 PACS number(s): 78.67.Ch, 73.22.Lp

I. INTRODUCTION

In carbon nanotubes, which are rolled-up two-dimensional (2D) graphite sheets, strong exciton effects emerge. They have been mainly studied by one-photon absorption. Two-photon absorption gives complementary information on excited excitons which are inaccessible by one-photon absorption. In this paper, we theoretically study the two-photon absorption spectrum of semiconducting carbon nanotubes within an effective-mass approximation including exciton effects.

Prominent effects of the Coulomb interaction on optical absorption in semiconducting carbon nanotubes were predicted.[1,2] The band gap is considerably enhanced and exciton binding energy is comparable to but slightly smaller than this enhancement. As a result, the intensity is focused on exciton energy levels in linear absorption spectra. This prediction was later confirmed both theoretically[3–8] and experimentally.[9–12] In recent experiments, possible absorption due to excited excitons was addressed.[13]

Two-photon absorption has also been studied.[14–21] The transition was shown to be prohibited between band edges in a one-particle model.[14] Photoluminescence experiments with two-photon absorption revealed that difference between the energies of one- and two-photon transitions is substantial, typically a few hundred meV, leading to the clear conclusion that the absorptions arise from excitons.[18–20] Moreover, calculations with exciton effects were performed and used for the estimation of exciton binding energy from experimental one- and two-photon peaks. Excited excitons were studied also by photoinduced absorption.[21]

In this paper, we present two-photon absorption spectra associated with exciton excited states for polarization parallel to the tube axis calculated systematically in an effective-mass approximation. The paper is organized as follows: In Sec. II, the model and method are briefly described. Numerical results are presented in Sec. III and discussed in Sec. IV. Summary and conclusion are given in Sec. V.

II. EFFECTIVE-MASS APPROXIMATION

In a 2D graphite sheet shown in Fig. 1(a), the conduction and valence bands consisting of π states cross at K and K' points and the electron motion around these points is described well by a $\mathbf{k}\cdot\mathbf{p}$ equation corresponding to a relativistic Dirac equation with vanishing rest mass. Around the K point, for example, it is given by[22–24]

$$\gamma(\vec{\sigma}\cdot\hat{\mathbf{k}})\mathbf{F}(\mathbf{r}) = \varepsilon\mathbf{F}(\mathbf{r}), \tag{1}$$

where $\mathbf{F}(\mathbf{r})$ is a two-component envelope function and the x and y coordinates are chosen in the circumference and the axis direction, respectively, as shown in Fig. 1(b), ε is an eigen energy, γ a band parameter, $\vec{\sigma}=(\sigma_x,\sigma_y)$ the Pauli-spin matrix, and $\hat{\mathbf{k}}\equiv -i\vec{\nabla}$ a wave vector operator.

Electronic states for a nanotube with a sufficiently large diameter are obtained by imposing the boundary condition around the circumference direction

$$\mathbf{F}(\mathbf{r}+\mathbf{L}) = \mathbf{F}(\mathbf{r})\exp\left(-\frac{2\pi i\nu}{3}\right), \tag{2}$$

with $\mathbf{L}$ being a chiral vector shown in Fig. 1(a) and ν an integer determined uniquely as $\nu=0$ or ± 1 through $n_a+n_b=3M+\nu$ with integer M, where n_a and n_b are integers defined by $\mathbf{L}=n_a\mathbf{a}+n_b\mathbf{b}$ and $\mathbf{a}$ and $\mathbf{b}$ are the primitive translation vectors shown in Fig. 1(a). The energy bands become

$$\varepsilon_{\pm,n}(k) = \pm\,\gamma\sqrt{\kappa_\nu(n)^2+k^2}, \tag{3}$$

where + and − denote the conduction and valence band, respectively, k is a wave vector in the axis direction, and

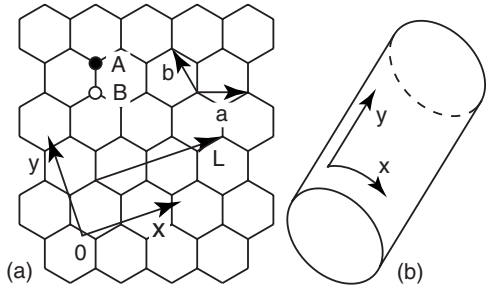

FIG. 1. Schematic illustration of (a) 2D graphite and (b) nanotube.

$$\kappa_\nu(n) = \frac{2\pi}{L}\left(n - \frac{\nu}{3}\right), \tag{4}$$

with integer n and $L=|\mathbf{L}|$. Around the K' point the $\mathbf{k}\cdot\mathbf{p}$ equation is given by Eq. (1) where $\vec{\sigma}$ is replaced by complex conjugate $\vec{\sigma}^*$. The boundary condition becomes Eq. (2) with replacement $\nu \to -\nu$.

A screened Hartree-Fock approximation is used for interaction effect on the band structure and an attractive electron-hole interaction is introduced by using the Coulomb interaction screened by a static dielectric function.[1,2] This approximation was shown to be sufficient by calculations in which dynamical effects are fully included[25,26] and used also for the study of exciton absorption in the cross-polarized geometry[27,28] and in metallic nanotubes.[29]

An exciton with the zero momentum is written as

$$|u\rangle = \sum_n \sum_k \psi_n^\mu(k) c_{+,n,k}^\dagger c_{-,n,k} |g\rangle, \tag{5}$$

where $c_{+,n,k}^\dagger$ and $c_{-,n,k}$ are the creation and annihilation operators, respectively, with $\pm$ indicating the conduction and valence bands and $|g\rangle$ is the ground state. Solving an equation of motion,[1,2] $\psi_n^\mu(k)$ and exciton energy ε_u are obtained. The wave function $\psi_n^\mu(k)$ is an even or odd function of k, that is,

$$\psi_n^\mu(-k) = \pm \psi_n^\mu(k). \tag{6}$$

In the following, we shall confine ourselves to the low-energy regime below the interband continuum and therefore completely neglect multiexciton states such as biexciton. For parallel polarization where the electric field is given by

$$E_x = 0, \quad E_y = E(e^{-i\omega t} + e^{i\omega t}), \tag{7}$$

a two-photon energy-absorption rate per unit length is given by $\beta(\omega)E^4$ with an absorption coefficient

$$\beta(\omega) = \frac{4\pi e^4}{\omega^3 A} \sum_{K,K'} \sum_u \left| \sum_{u'} \frac{\langle u|\hat{v}_y|u'\rangle\langle u'|\hat{v}_y|g\rangle}{\hbar\omega - \varepsilon_{u'}} \right|^2 \delta(2\hbar\omega - \varepsilon_u), \tag{8}$$

where $\hat{v}_y$ is a velocity operator in the axis direction. Using typical scales of physical quantities in nanotubes, a dimensionless absorption coefficient $\bar{\beta}(\omega)$ is given by

$$\beta(\omega) = \frac{e^4 L^5}{8\pi^3 \hbar \gamma^2} \bar{\beta}(\omega). \tag{9}$$

Then, we can see that the absorption coefficient is proportional to the fifth power of the circumference length.

The velocity matrix elements for the K point are given by

$$\langle u'|\hat{v}_y|g\rangle = \frac{i\gamma}{\hbar} \sum_n \sum_k \frac{\kappa_\nu(n)}{\sqrt{\kappa_\nu(n)^2 + k^2}} \psi_n^{\mu'}(k)^*, \tag{10}$$

and

$$\langle u|\hat{v}_y|u'\rangle = -\frac{2\gamma}{\hbar} \sum_n \sum_k \frac{k}{\sqrt{\kappa_\nu(n)^2 + k^2}} \psi_n^\mu(k)^* \psi_n^{\mu'}(k). \tag{11}$$

Those for the K' point are given by the complex conjugate of the above with the replacement $\nu \to -\nu$. It can be seen from Eqs. (10) and (11) that states with even parity are excited from the ground state by one-photon absorption and those with odd parity are excited by two-photon absorption. This selection rule obtained within the effective-mass scheme corresponds to the more general rule based on the symmetry under the π rotation around the center of a carbon-atom hexagon obtained previously.[19,21,30]

The strength of the Coulomb interaction is characterized by dimensionless parameter $(e^2/\kappa L)(2\pi\gamma/L)^{-1}$, which is the ratio of the typical Coulomb energy $e^2/\kappa L$ and the typical kinetic energy $2\pi\gamma/L$, where κ is an effective dielectric constant. The band parameter is related to hopping integral γ_0 through $\gamma = (\sqrt{3}/2)a\gamma_0$ with lattice constant $a = 2.46$ Å in a nearest-neighbor tight-binding model. For a rough estimate of the interaction strength, we can use this relation with $\gamma_0 \sim 3$ eV and then have $(e^2/\kappa L)(2\pi\gamma/L)^{-1} \sim 0.35/\kappa$. The dielectric constant κ describes effects of screening by electrons in σ bands, core states, and the π bands away from the K and K' points and by the surrounding material if any. Its exact value is not known, but we can expect that κ is not so much different from 2.4 in bulk graphite. Then, the interaction parameter lies roughly in the range $0.1 \sim 0.2$.

The band parameter γ is related to the Fermi velocity $v_F = \gamma/\hbar$ in 2D graphite sheet, which is likely to be renormalized by electron-electron interaction. The part of the renormalization due to interactions with electrons in the vicinity of the K and K' points should be excluded in the present scheme, and therefore the relation $\gamma = (\sqrt{3}/2)a\gamma_0$ is not strictly valid for a commonly used value of γ_0 containing interaction effects. As will be shown below, we should set $\gamma_0 \approx 2.7$ eV in order to reproduce observed one- and two-photon absorption energies in semiconducting nanotubes, suggesting that the velocity renormalization is not so significant. It is worth being pointed out that the interaction parameter is related to "fine-structure constant" $\alpha = e^2/\hbar v_F$ through $(e^2/\kappa L)(2\pi\gamma/L)^{-1} = \alpha/(2\pi\kappa)$.

The infinitely extending energy bands in Eq. (3) should be cut off by an energy ε_c of the order of the half of the π-band width $3\gamma_0$. Therefore, $\varepsilon_c(2\pi\gamma/L)^{-1} \approx (\sqrt{3}/\pi)(L/a) = \sqrt{3}d/a$, with d being the diameter of the nanotube. Since excitation energy exhibits only weak dependence on the cutoff energy,[2] we use a typical value $\varepsilon_c(2\pi\gamma/L)^{-1} = 10$ corresponding to diameter ~ 1.4 nm in the following unless specified otherwise. It should be noted for use of the following results that the kinetic energy $2\pi\gamma/L$ which is used as energy units is about 1 eV for tubes with typical diameter $d \sim 1.4$ nm.

III. NUMERICAL RESULTS

Typical examples of energy dependence of two-photon absorption coefficient are shown in Fig. 2 where energy broadening is introduced by using a Lorentzian function with a half width at half maximum Γ. In Fig. 2(a), the Coulomb interaction is absent, in Fig. 2(b) the self-energy is included for $(e^2/\kappa L)(2\pi\gamma/L)^{-1} = 0.1$ and 0.2 while the electron-hole interaction is not, and in Figs. 2(c) and 2(d), both of them are considered for $(e^2/\kappa L)(2\pi\gamma/L)^{-1} = 0.1$ and 0.2, respectively. The lowest band edge is shown by downward arrows. In

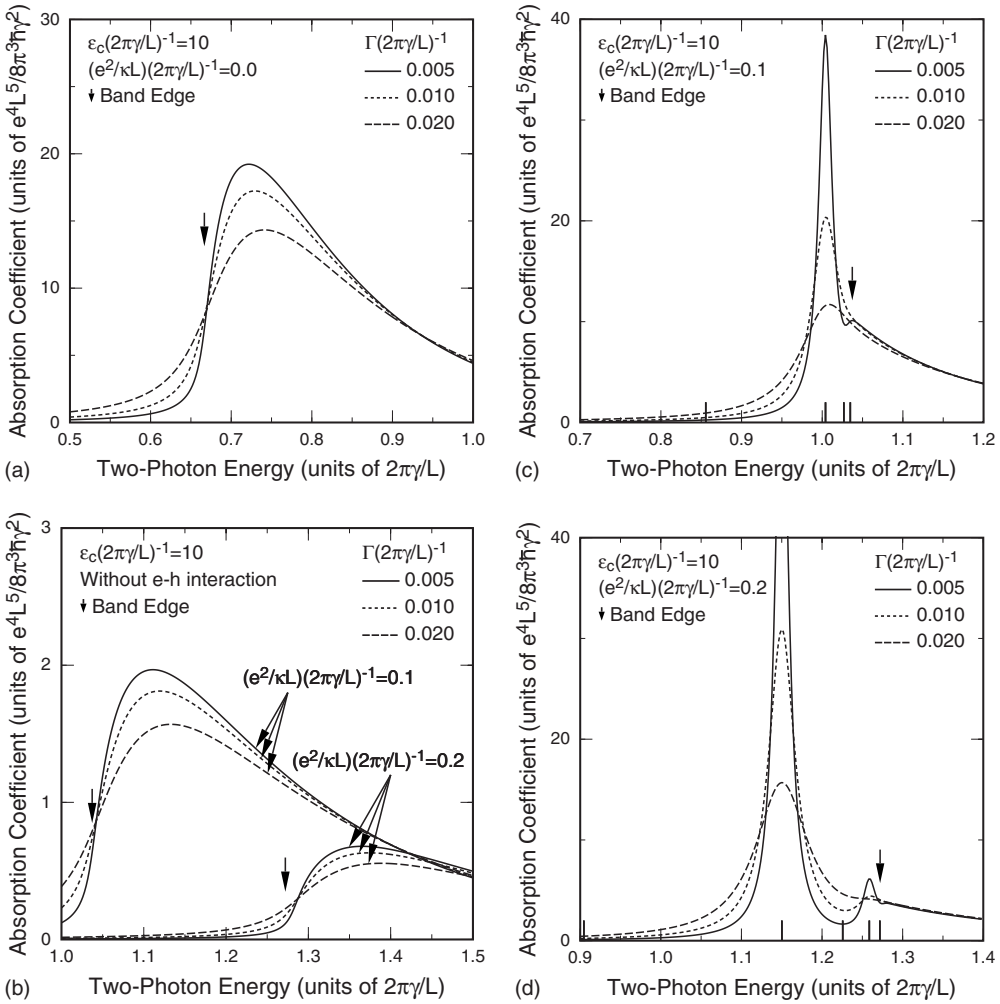

FIG. 2. Calculated two-photon absorption coefficient. In (a), $(e^2/\kappa L)(2\pi\gamma/L)^{-1}=0$, in (b) the self-energy is included for $(e^2/\kappa L)(2\pi\gamma/L)^{-1}=0.1$ and 0.2 while the electron-hole interaction is absent, and in (c) and (d), both of them are taken into account for $(e^2/\kappa L)(2\pi\gamma/L)^{-1}=0.1$ and 0.2, respectively. Phenomenological broadening $\Gamma(2\pi\gamma/L)^{-1}$ is introduced. The arrows indicate the band edge and the short vertical lines at the bottom of (c) and (d) denote exciton energies.

Figs. 2(c) and 2(d), the energy of all the exciton bound states is indicated by short vertical lines at the bottom.

In Fig. 2(a), the spectrum in the absence of the interaction shows a broad peak above the band edge. The deviation of the peak position from the band edge is due to vanishing velocity matrix element at $k=0$ as shown in Eq. (11).[14] This means that even in the absence of the interaction, there is a finite difference of peak positions $\sim 0.04\times(2\pi\gamma/L)$ between one- and two-photon absorption spectra because the one-photon peak is exactly at the band edge due to the strong van Hove singularity. It is noted that the wave-number dependence of Γ which can lead to absorption at the band edge[14] is not considered.

In Fig. 2(b), essential features are same as those in Fig. 2(a). The self-energy enhances the band gap[1,2] and suppressed intensity in comparison with the previous result comes from the factor ω^{-3} in Eq. (8). Deviations of the peak positions for $(e^2/\kappa L)(2\pi\gamma/L)^{-1}=0.1$ and 0.2 from the band edges are about 0.06 and 0.08, respectively, in units of $2\pi\gamma/L$ which are typically 60 and 80 meV for $d\sim 1.4$ nm and larger than experimental accuracy of a few meV.[31] Shift of the peaks due to the energy broadening is approximately in proportion to Γ with a coefficient of the order of unity.

When the electron-hole interaction is introduced, a prominent peak appears corresponding to the second lowest exciton with odd parity in Figs. 2(c) and 2(d) and another peak associated with the fourth lowest exciton appears in Fig. 2(d). The difference between the first and second lowest exciton energies is approximately 0.15 and 0.22 in units of $2\pi\gamma/L$ for $(e^2/\kappa L)(2\pi\gamma/L)^{-1}=0.1$ and 0.2, respectively, which are 0.15 and 0.22 eV, respectively, for $d\sim 1.4$ nm. They are about 2.5 and 2.8 times, respectively, as large as the difference between peak positions of one- and two-photon absorptions in the absence of the electron-hole interaction in Fig. 2(b).

In Fig. 3, the Coulomb-interaction dependence of the exciton energies is shown. Solid and dotted lines denote excitons contributing to one- and two-photon absorption spectra, respectively. With increase of the interaction, many exciton bound states split off from the interband continuum. Similar results were previously reported for a different cutoff energy.[1]

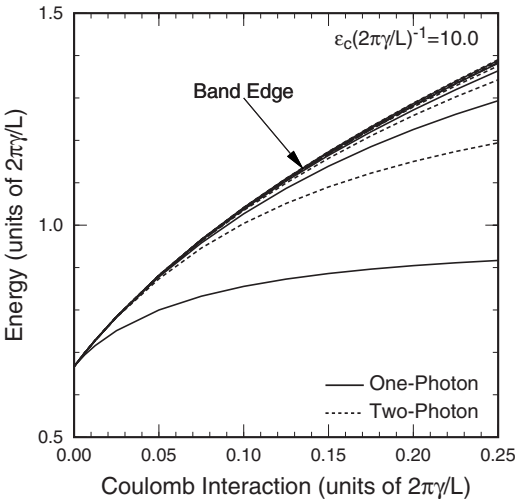

FIG. 3. Coulomb-interaction dependence of exciton energies associated with the lowest band. Solid and dotted lines denote excitons excited by one- and two-photon absorptions, respectively.

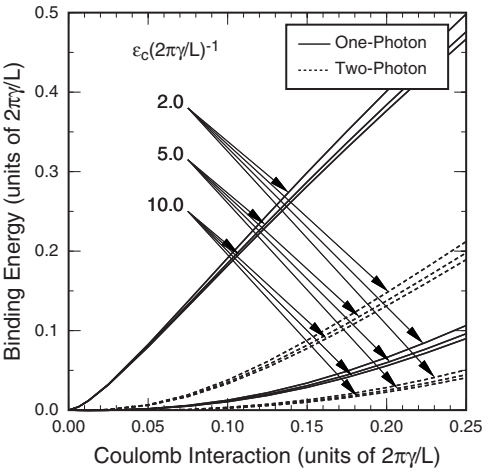

FIG. 4. Coulomb-interaction dependence of the binding energies of the lowest four excitons. The cutoff energy is chosen as $\varepsilon_c(2\pi\gamma/L)^{-1}=2$, 5, and 10.

Figure 4 shows the binding energies of the lowest four excitons and for cutoff energy $\varepsilon_c(2\pi\gamma/L)^{-1}=2$, 5, and 10. The binding energy slightly decreases with the increase of the cutoff energy mainly because the screening effects increase with the increase of the cutoff.[2] The binding energies of the first and second lowest excitons are of the same order for $(e^2/\kappa L)(2\pi\gamma/L)^{-1}=0.1\sim0.2$. The ratio of the energy of the second lowest exciton state to that of the ground state is about 0.2 and 0.35 for $(e^2/\kappa L)(2\pi\gamma/L)^{-1}=0.1$ and 0.2, respectively, comparable to that in a three-dimensional (3D) hydrogenic model.

In a hydrogen atom, the ratio of the binding energy of the first-excited state to that of the ground state is exactly 1/4. This fact is usually used for the determination of the exciton binding energy in bulk semiconductors from one- and two-photon absorption energies. In 2D the exciton energies are given by $\propto[n-(1/2)]^{-2}$ with $n=1,2,\ldots$.[32] Because of the small kinetic energy in lower dimensions, the ground-state energy is lowered considerably in comparison with excited states and the ratio is reduced to 1/9. In one-dimension (1D) hydrogenic model, the ground-state energy becomes infinite because of the infinitely large attractive potential at the origin.[33,34] This divergence is cut off by a nonzero width or diameter in quasi-1D systems. It is expected, therefore, that the ratio is further reduced in carbon nanotubes if the screening effects are not considered.

Actually, the excited states have a binding energy not so much smaller than the ground state in carbon nanotubes. This is due to the screening property of low dimensional systems as discussed previously.[35] A static dielectric function for wave vector q is given by

$$\varepsilon(q) = 1 + V(q)\Pi(q), \tag{12}$$

where $V(q)$ is the Fourier transform of the Coulomb potential and $\Pi(q)$ a static polarization function. The Coulomb potential becomes $4\pi e^2/\kappa q^2$ in 3D, $2\pi e^2/\kappa q$ in 2D, and $(2e^2/\kappa A)K_0(Lq/2\pi)I_0(Lq/2\pi)$ ($\propto -\ln q$ for small q) in nanotubes,[1] where $K_n(z)$ and $I_n(z)$ are the modified Bessel functions of the nth order. Since in a limit of $q\to0$, $\Pi(q)\propto q^2$ for all the cases with nonvanishing gap, the screening in the large distance remains constant for 3D while it disappears for 2D and 1D nanotubes. This can be understood by the fact that most of the electric flux lines go through the outer space instead of the quasi-2D and quasi-1D systems. In nanotubes, therefore, excitons in excited states are subjected to strong attractive force and lowered in energy.

In Fig. 5, the intensity of the two-photon absorption coefficient is shown as a function of the interaction strength. The intensity is defined as a half of the factor in front of the delta function in Eq. (8). Solid and dotted lines are results for the second and fourth lowest excitons, respectively. The intensity decreases with increase of the cutoff energy because of the cutoff-energy dependence of the screening effects as mentioned above. The dotted line is nearly 10% of the solid line for $(e^2/\kappa L)(2\pi\gamma/L)^{-1}=0.1\sim0.2$ and $\varepsilon_c(2\pi\gamma/L)^{-1}=10$.

As shown in Fig. 4, the binding energy of the fourth lowest exciton for $d\sim1.4$ nm is about 2 and 20 meV for

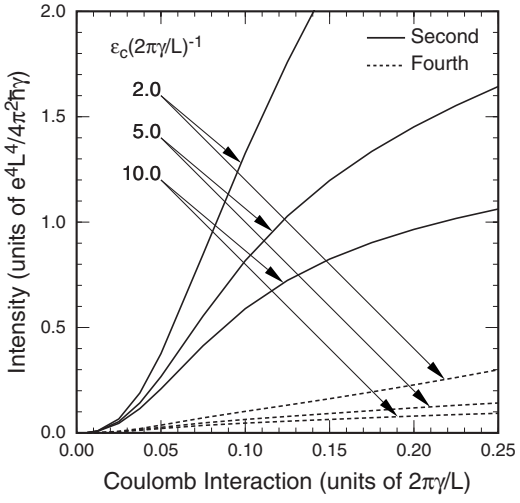

FIG. 5. Coulomb-interaction dependence of the intensity of the two-photon absorption coefficient. Solid and dashed lines denote the second and fourth lowest excitons, respectively.

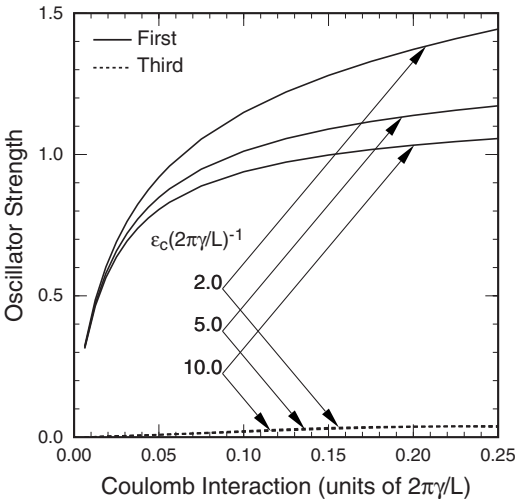

FIG. 6. Coulomb-interaction dependence of the oscillator strength of the dynamical conductivity. Solid and dashed lines denote the first and third lowest excitons, respectively.

$(e^2/\kappa L)(2\pi\gamma/L)^{-1}=0.1$ and 0.2, respectively, which can be larger than experimental accuracy and energy broadening at low temperature of a few meV.[31] Therefore, the above suggests that the fourth lowest exciton may be observed by two-photon absorption when its energy is well resolved from the interband continuum.

Figure 6 shows the oscillator strength[2] of the one-photon absorption. The results for the ground and third lowest excitons are plotted by solid and dotted lines, respectively. The oscillator strength of the third lowest exciton is only about 2%–3% of that of the lowest exciton in the range from $(e^2/\kappa L)(2\pi\gamma/L)^{-1}=0.1$ to 0.2 for $\varepsilon_c(2\pi\gamma/L)^{-1}=2$, 5, and 10, although it has an appreciable binding energy. This suggests that observation of this exited exciton requires very high accuracy.

IV. DISCUSSION

In Fig. 7, excitation energies are plotted as a function of the circumference length. Solid and dotted lines denote calculated energies of the two lowest excitons observable in one- and two-photon absorptions, respectively, and dashed lines indicate band edges. Symbols are experimental results[19,20] where open and filled symbols indicate excitons for one- and two-photon transitions, respectively. We have set $\gamma_0 \approx 2.7$ eV which was used for comparison with experiments for the lowest excitons associated with the first and second gaps in a previous paper.[2]

As shown in Fig. 3, the energy of the lowest exciton is weakly dependent on the interaction strength $(e^2/\kappa L)(2\pi\gamma/L)^{-1}$. Therefore, the band parameter is uniquely determined as approximately $\gamma_0 \approx 2.7$ eV. Using the position of the second exciton, strongly dependent on the Coulomb interaction, we can place the interaction parameter in the range $0.1 < (e^2/\kappa L)(2\pi\gamma/L)^{-1} < 0.2$. For $d \sim 1$ nm, for example, the binding energy of the lowest exciton changes from ~0.21 to ~0.43 eV in this interaction range. More precise determination becomes possible when we include other effects such as a higher order $\mathbf{k}\cdot\mathbf{p}$ term giving trigonal warping, curvature, and lattice distortions,[2] leading to a family effect observed experimentally.[11,12]

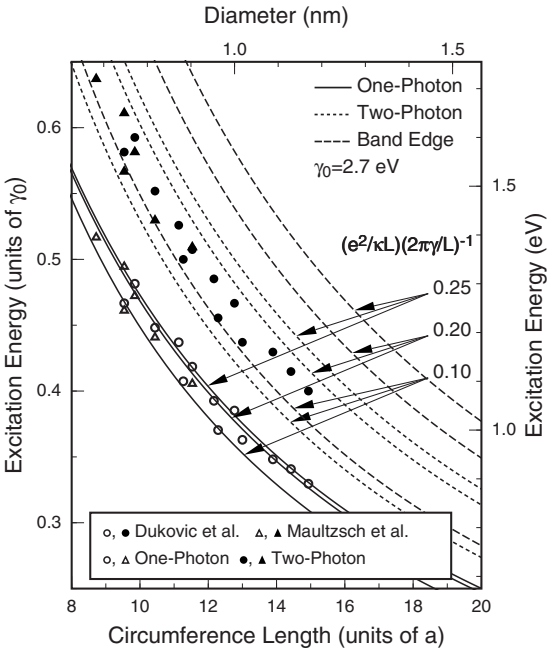

FIG. 7. Calculated excitation energies as a function of the circumference length. Solid and dotted lines denote the energies for one- and two-photon absorptions, respectively, and dashed lines are the band edges. Symbols denote experimental results (Refs. 19 and 20) where open and closed symbols indicate one- and two-photon transitions, respectively.

It is worth mentioning that some corrections to the present model of constant κ can appear more effectively for excited excitons than for the lowest exciton. As has already been discussed, the screening property is quite different between the lowest and excited excitons due to the distribution of electric flux lines. This may be applicable to minor screening due to electrons in bands other than the π states and screening due to the surrounding material if any. This means that more precise modeling of the Coulomb interaction may be required for detailed comparison between theory and experiments. This is out of the scope of this paper and left for a future study.

In recent photoluminescence measurements,[13] peaks denoted by L_1 and L_1^* appear higher than two-photon peaks with intensity about one-order-of-magnitude smaller than that of the exciton of the second band. In the present results for $\gamma_0 \approx 2.7$ eV, these peaks lie in the interband continuum and around the band edge for $(e^2/\kappa L)(2\pi\gamma/L)^{-1} \sim 0.1$ and ~0.25, respectively.

V. SUMMARY AND CONCLUSION

We have studied two-photon absorption spectra associated with excited exciton states of semiconducting carbon nanotubes for parallel polarization within the effective-mass approximation. Two-photon exciton peaks appear at energies of the second and fourth lowest levels with odd parity. Typi-

cally, the binding energy of the second lowest exciton approximately lies between 20% and 40% of that of the lowest exciton depending on the strength of the Coulomb interaction. The theory is in good agreement with experiments for the interaction strength $(e^2/\kappa L)(2\pi\gamma/L)^{-1}$ lying between 0.1 and 0.2 apart from a family effect not included in the present scheme.

ACKNOWLEDGMENTS

This work was supported in part by a 21st Century COE Program at Tokyo Tech "Nanometer-Scale Quantum Physics," Grants-in-Aid for Scientific Research, and Grant-in-Aid for Scientific Research on Priority Area "Carbon Nanotube Nanoelectronics" from the Ministry of Education, Culture, Sports, Science, and Technology, Japan.

[1] T. Ando, J. Phys. Soc. Jpn. **66**, 1066 (1997).
[2] T. Ando, J. Phys. Soc. Jpn. **73**, 3351 (2004).
[3] C. D. Spataru, S. Ismail-Beigi, L. X. Benedict, and S. G. Louie, Phys. Rev. Lett. **92**, 077402 (2004).
[4] C. D. Spataru, S. Ismail-Beigi, R. B. Capaz, and S. G. Louie, Phys. Rev. Lett. **95**, 247402 (2005).
[5] E. Chang, G. Bussi, A. Ruini, and E. Molinari, Phys. Rev. Lett. **92**, 196401 (2004).
[6] V. Perebeinos, J. Tersoff, and Ph. Avouris, Phys. Rev. Lett. **92**, 257402 (2004).
[7] H. Zhao and S. Mazumdar, Phys. Rev. Lett. **93**, 157402 (2004).
[8] C. L. Kane and E. J. Mele, Phys. Rev. Lett. **93**, 197402 (2004).
[9] M. Ichida, S. Mizuno, Y. Tani, Y. Saito, and A. Nakamura, J. Phys. Soc. Jpn. **68**, 3131 (1999).
[10] M. Ichida, S. Mizuno, Y. Saito, H. Kataura, Y. Achiba, and A. Nakamura, Phys. Rev. B **65**, 241407(R) (2002).
[11] M. J. O'Connell, S. M. Bachilo, C. B. Huffman, V. C. Moore, M. S. Strano, E. H. Haroz, K. L. Rialon, P. J. Boul, W. H. Noon, C. Kittrell, J. Ma, R. H. Hauge, R. B. Weisman, and R. E. Smalley, Science **297**, 593 (2002).
[12] S. M. Bachilo, M. S. Strano, C. Kittrell, R. H. Hauge, R. E. Smalley, and R. B. Weisman, Science **298**, 2361 (2002).
[13] J. Lefebvre and P. Finnie, Phys. Rev. Lett. **98**, 167406 (2007).
[14] Vl. A. Margulis and T. A. Sizikova, Physica B (Amsterdam) **245**, 173 (1998).
[15] Vl. A. Margulis and E. A. Gaiduk, J. Opt. A, Pure Appl. Opt. **3**, 267 (2001).
[16] E. J. Mele, P. Kral, and D. Tomanek, Phys. Rev. B **61**, 7669 (2000).
[17] W.-D. Cheng, D.-S. Wu, X.-D. Li, Y.-Z. Lan, H. Zhang, D.-G. Chen, Y.-J. Gong, Y.-C. Zhang, F.-F. Li, J. Shen, and Z.-G. Kan, Phys. Rev. B **70**, 155401 (2004).
[18] F. Wang, G. Dukovic, L. E. Brus, and T. F. Heinz, Science **308**, 838 (2005).
[19] J. Maultzsch, R. Pomraenke, S. Reich, E. Chang, D. Prezzi, A. Ruini, E. Molinari, M. S. Strano, C. Thomsen, and C. Lienau, Phys. Rev. B **72**, 241402(R) (2005).
[20] G. Dukovic, F. Wang, D. Song, M. Y. Sfeir, T. F. Heinz, and L. E. Brus, Nano Lett. **5**, 2314 (2005).
[21] H. Zhao, S. Mazumdar, C.-X. Sheng, M. Tong, and Z. V. Vardeny, Phys. Rev. B **73**, 075403 (2006).
[22] H. Ajiki and T. Ando, J. Phys. Soc. Jpn. **62**, 1255 (1993).
[23] T. Ando, J. Phys. Soc. Jpn. **74**, 777 (2005).
[24] J. C. Slonczewski and P. R. Weiss, Phys. Rev. **109**, 272 (1958).
[25] H. Sakai, H. Suzuura, and T. Ando, J. Phys. Soc. Jpn. **72**, 1698 (2003).
[26] H. Sakai, H. Suzuura, and T. Ando, Physica E (Amsterdam) **22**, 704 (2004).
[27] S. Uryu and T. Ando, Phys. Rev. B **74**, 155411 (2006).
[28] S. Uryu and T. Ando, Phys. Rev. B **76**, 115420 (2007).
[29] S. Uryu and T. Ando, Phys. Rev. B **77**, 205407 (2008).
[30] M. Damnjanović, I. Milošević, T. Vuković, and R. Sredanović, Phys. Rev. B **60**, 2728 (1999).
[31] K. Matsuda, T. Inoue, Y. Murakami, S. Maruyama, and Y. Kanemitsu, Phys. Rev. B **77**, 033406 (2008).
[32] T. Ando, A. B. Fowler, and F. Stern, Rev. Mod. Phys. **54**, 437 (1982), and references cited therein.
[33] R. Loudon, Am. J. Phys. **27**, 649 (1959).
[34] R. J. Elliott and R. Loudon, J. Phys. Chem. Solids **8**, 382 (1959); **15**, 196 (1960).
[35] F. Wang, D. J. Cho, B. Kessler, J. Deslippe, P. J. Schuck, S. G. Louie, A. Zettl, T. F. Heinz, and Y. R. Shen, Phys. Rev. Lett. **99**, 227401 (2007).